Energy 56 (2013) 108–116

Contents lists available at SciVerse ScienceDirect

Energy

journal homepage: www.elsevier.com/locate/energy

Super-adiabatic combustion in Al_2O_3 and SiC coated porous media for thermoelectric power conversion

Kyle T. Mueller [a], Oliver Waters [a], Valeri Bubnovich [b], Nina Orlovskaya [a,*], Ruey-Hung Chen [a]

[a] Department of Mechanical and Aerospace Engineering, University of Central Florida, 4000 Central Florida Blvd., Orlando, FL 32816-2450, USA
[b] Department of Chemical Engineering, Universidad de Santiago de Chile, B. O'Higgins 3363, Santiago, Chile

ARTICLE INFO

Article history:
Received 6 November 2012
Received in revised form
26 April 2013
Accepted 27 April 2013
Available online 28 May 2013

Keywords:
Super-adiabatic combustion
Porous media burner
Thermoelectrics
Power conversion
Low-calorific fuel

ABSTRACT

The combustion of ultra-lean fuel/air mixtures provides an efficient way to convert the chemical energy of hydrocarbons and low-calorific fuels into useful power. Matrix-stabilized porous medium combustion is an advanced technique in which a solid porous medium within the combustion chamber conducts heat from the hot gaseous products in the upstream direction to preheat incoming reactants. This heat recirculation extends the standard flammability limits, allowing the burning of ultra-lean and low-calorific fuel mixtures and resulting a combustion temperature higher than the thermodynamic equilibrium temperature of the mixture (i.e., super-adiabatic combustion). The heat generated by this combustion process can be converted into electricity with thermoelectric generators, which is the goal of this study.

The design of a porous media burner coupled with a thermoelectric generator and its testing are presented. The combustion zone media was a highly-porous alumina matrix interposed between upstream and downstream honeycomb structures with pore sizes smaller than the flame quenching distance, preventing the flame from propagating outside of the central section. Experimental results include temperature distributions inside the combustion chamber and across a thermoelectric generator; along with associated current, voltage and power output values. Measurements were obtained for a catalytically inert Al_2O_3 medium and a SiC coated medium, which was tested for the ability to catalyze the super-adiabatic combustion. The combustion efficiency was obtained for stoichiometric and ultra-lean (near the lean flammability limit) mixtures of CH_4 and air.

1. Introduction

Matrix-stabilized porous burner technology is an advanced combustion method in which a mixture of fuel and oxidizer is burned within a solid porous medium, providing favorable conditions for the combustion of lean mixtures. The solid porous medium provides a mechanism of heat recirculation where the high temperature combustion products in the post-flame zone heat the upstream porous solid which, in turn, preheats the incoming reactants, [1–4], where the comprehensive review of the combustion in porous media is provided in Ref. [1], a modeling of combustion in side of the porous media presented in Ref. [2], design and operation of the porous burner described in Ref. [3], porous media compact heat exchanger is investigated in Ref. [4]. The process results in a flame temperature higher than the equilibrium adiabatic value achievable by the fuel–oxidizer mixture in the absence of a porous medium. This process is called super-adiabatic combustion [5–9]. A porous medium with a very large surface-area-to-volume ratio increases contact of the solid and gas, thus maximizing the heat transfer between the solid and gas phases [7,10,11]. Such a heat transfer mechanism is absent in a typical gas burner. The heat transfer is further enhanced by the dispersion of the gases flowing through the porous medium and the mixing due to turbulence generated by the presence of the solid medium [2,8]. Fig. 1 shows a schematic presentation of a three-section porous burner. The flame is stabilized and localized within the central high-porosity section interposed between two lower-porosity honeycomb sections that serve to quench the flame if it propagates upstream or downstream of the central section.

Because porous burners are advantageous for sustaining lean flames, they are also desirable for burning low-calorific gases [12,13]. Among possible practical applications of porous burner

* Corresponding author. Tel.: +1 407 823 5770; fax: +1 407 823 0802.
E-mail address: Nina.Orlovskaya@ucf.edu (N. Orlovskaya).

0360-5442/$ – see front matter © 2013 Elsevier Ltd. All rights reserved.
http://dx.doi.org/10.1016/j.energy.2013.04.068

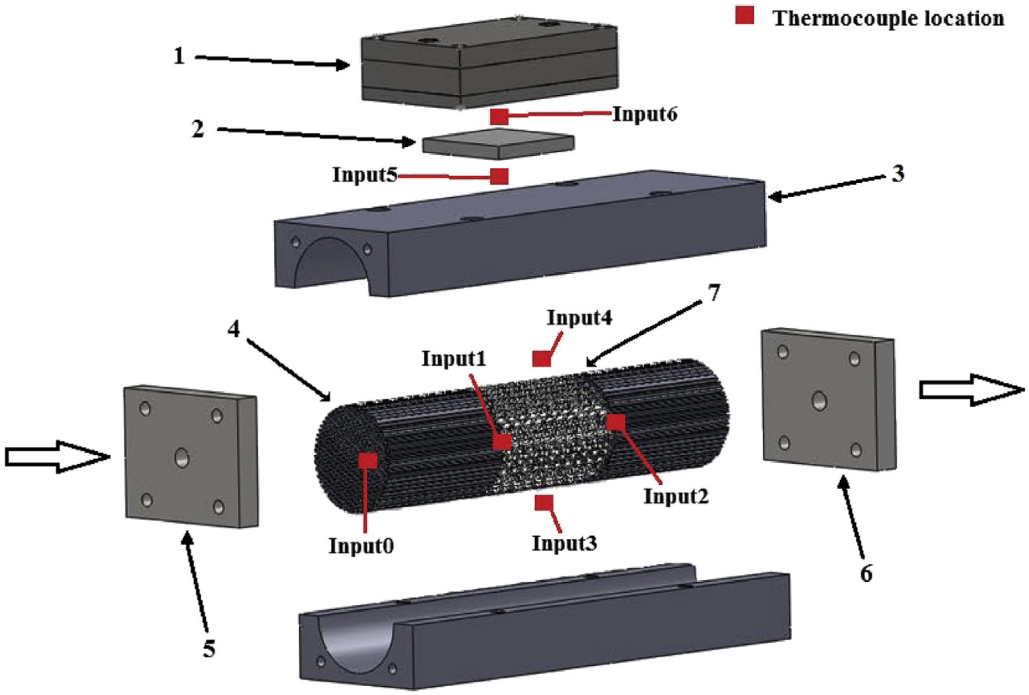

Fig. 1. Schematic of porous burner assembly; 1 – Air cooling system, 2 – Thermoelectric device, 3 – Metallic casing, 4 – Low porosity section, 5 – Reactant inlet plate, 6 – Exhaust side plate, 7 – High-porosity section. The arrows point out on the specific parts of the assembly.

technology are power generation via thermoelectric devices [9,14–16], small scale heating purposes [17], and combustion of low-calorific value landfill-seepage gases [3,18].

Thermoelectric generators operate by utilizing the Seebeck effect: a temperature difference across two joined, but different, conducting materials will create a voltage [19]. In order to further increase the voltage and power output, the temperature difference may be increased by increasing the hot-side temperature and/or decreasing the cool-side temperature across the device. Therefore, for a burner utilizing thermoelectric devices, the power generated can be maximized by increasing the combustion temperature, and/or by cooling the cool-side of the device through either passive means, like a heat-sink, or active means, like a fan or impinging air jet. It is a standard practice to connect multiple thermoelectric devices together in series to increase the voltage and power outputs, as was already done in most commercially-available thermoelectric devices [19]. The discussed burner prototype design uses an impinging jet of air to cool the cool-side of the thermoelectric device while the hot-side of the thermoelectric module is mounted directly on the surface of the metallic casing to regulate the temperature in the combustion zone down to an acceptable amount below the temperature limit of the thermoelectric material. The use of a porous medium burner coupled with thermoelectrics has the potential to provide a reliable source of power.

The goal of this research is to report (i) the design of the porous burner and (ii) test its performance using both inert and catalytically active porous media for combustion as well as (iii) utilizing thermoelectric modules to collect electric power. The comparison of porous burner performance using alumina and silicon carbide coated porous media was used to find out if catalytically active SiC would provide advantages over catalytically inert Al_2O_3 porous matrices.

2. Design of porous burner

Special consideration must be given to the configuration design and material selection for the porous burner to avoid easy degradation and maximize the heat transfer capabilities. The photograph of assembled porous burner ready for operation is shown in Fig. 2A. Good heat transfer properties of the solid medium allow the burning of lean mixtures, maintain a homogeneous maximum flame temperature over the length of the combustion zone, and allow time for CO oxidation [10,20–22] which helps to lower air pollution. Because the power conversion using thermoelectric effect is proportional to the surface area of the device, it is desirable to have high temperatures over the entire length of the burner.

Solid porous media could be made as reticulated foam, a packed bed of spheres or saddles, thin wire mesh, foil, or even an ordered structure such as a honeycomb [23,24]. In comparison with other porous media, foams exhibit much better convective heat transfer due to their large internal surface area. Foams have the additional advantage of being easily manufacturable in a variety of complex shapes [12]. Packed beds of ceramic spheres or saddles have somewhat worse heat transfer characteristics than foams due to poor heat transfer (i.e., extra contact thermal resistances) between individual elements [1,12,25]. Wire meshes and foils are problematic due to thermal degradation at high temperatures, in addition to extra thermal resistances [12,25]. The porous foam material in the burner can be catalytically inert, such as alumina, quartz or zirconia, and may be coated with a catalytically active material to help facilitate the combustion process, [1,26,27] especially for ultra-lean or low-calorific mixtures. A catalytically coated ceramic foam/porous matrix is, therefore, highly desirable.

One of the most broadly used materials for the combustion section is porous alumina [10,11,13]. It is known that alumina does not exhibit catalytic properties to facilitate fuel oxidation and oxygen reduction to promote combustion, but it has a lot of advantages: such as easy manufacturability, high mechanical strength, low cost, and broad availability. The parameters of alumina used as a media in super-adiabatic combustion are the size of pores typically in the range of 1–2 mm and porosity level at 80–85%, in order to provide the best environment for combustion [5,18,28]. Thus, in the proposed design of the central combustion section of the porous burner, commercially-available highly-porous (80%)

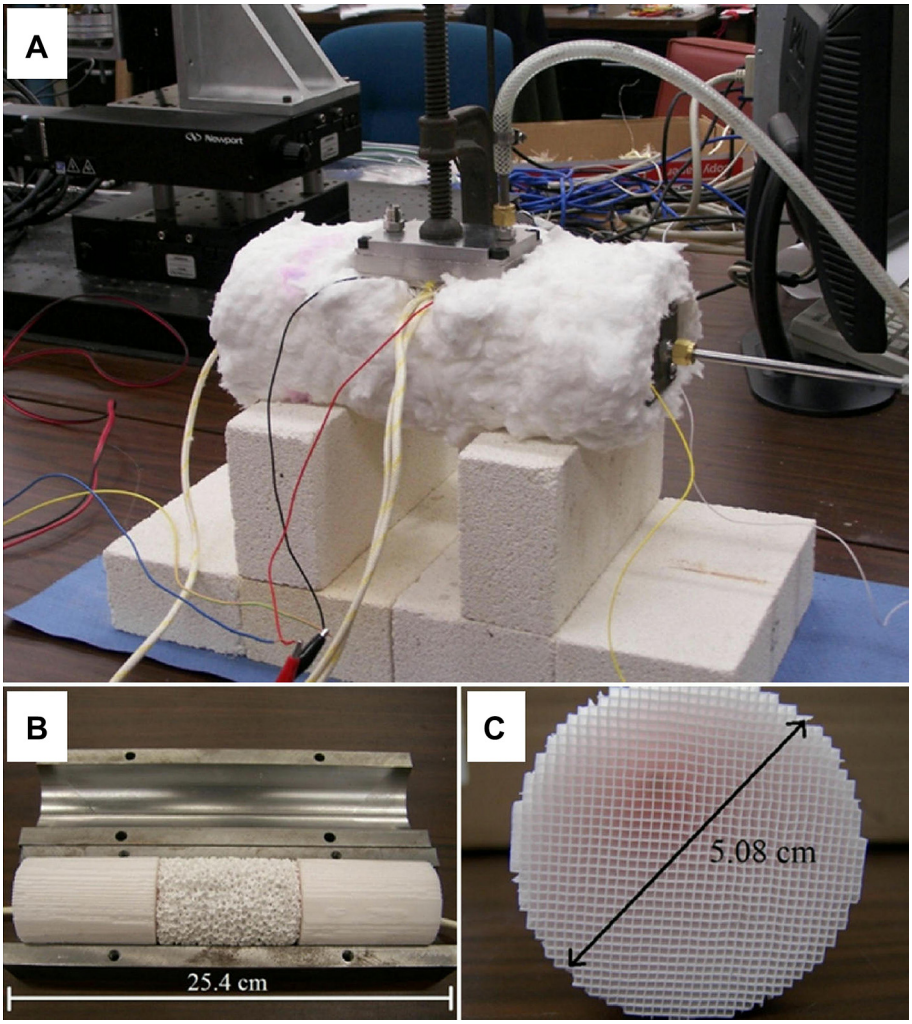

Fig. 2. Top: Picture of proof-of-concept burner prototype; Bottom left: the burner configuration with a central high-porosity ceramic foam section and two outer low-porosity honeycomb sections resting in a metallic casing. Bottom right: an end view of one of the low-porosity side sections.

alumina is used (Fig. 2B), while the upstream and downstream sections contain honeycomb alumina structures with 62 pores/cm^2 porosity, shown in Fig. 2B and C. The highly-porous alumina part had a 5.08 cm diameter and a 7.62 cm length, and was used as a combustion chamber in the central section of the porous burner (Fig. 2B). The honeycomb alumina media with a 62 pores/cm^2 porosity used in the upstream and downstream sections are shown in Fig. 2B and C. The two honeycomb sections have a pore size smaller than the quenching distance, serving to prevent flame propagation in either the upstream or downstream direction and to stabilize the combustion zone within the central alumina section.

The final design of the porous media burner for super-adiabatic combustion is shown in Fig. 1 and it includes the following components:

- A rectangular steel casing with a cylindrical interior to house the porous sections.
- A highly-porous pure alumina (99.5 wt% Al_2O_3) reticulated foam (76.2 mm long and 50.8 mm in diameter, porosity of 80%, 20 ppi) that will contain the flame as the central section and transport heat to the casing (Manufacturer: Süd-Chemie Hi-Tech Ceramics, Louisville, KY).
- Two lower-porosity alumina honeycomb sections (62 pores/cm^2) before and after the central section to keep the flame confined (Manufacturer: Applied Ceramics, Laurens, SC).
- A thermoelectric device to harvest the heat released by combustion. The current work uses a commercially-available Bi_2Te_3 alloy module. It has a maximum no-load power output of 7.95 W and hot-side temperature limit of 250 °C and 4.97% conversion efficiency (Model number TG 12-8-01-L; Manufacturer: Marlow Industries, Inc., Dallas, TX).
- An impinging jet manifold to cool the cool-side of the thermoelectric to maximize the temperature difference, and therefore power output, of the thermoelectric module.
- The flow controllers used to measure the incoming air and fuel flows are OMEGA FMA-3206 models (Manufacturer: OMEGA Engineering Inc., Stanford, CT).
- The filter used for the reactant air flow is a 9.5 mm NPT (F) Air Line Filter (Manufacturer: Ingersoll Rand, Davidson, NC).
- The variable voltage sources used as inputs to the flow controllers are GW INSTEK PSS-2005 Programmable Power Supplies (Manufacturer: Good Will Instrument Co., Ltd, Chino, CA).
- The data acquisition system used is an USB-6210 16 inputs 16-bit 250 kS/s Multifunction I/O (Manufacturer: National Instruments, Austin, TX).
- Eight type-K insulated thermocouples to obtain an accurate temperature measurements within the burner and to measure the temperature difference across the thermoelectric module (Manufacturer: OMEGA, #XC-K-24-25, 24awg gauge, rated to 1200 °C, Standford, CT).

- KLINGERsil Milam Laminate, Type PSS, high temperature, 870 °C, gasket material is used between the joining sections of the casing (Manufacturer: Macroseal, Inc., Hopewell, VA).
- Durablanket S type insulation was used, made from spun ceramic fibers, rated up to 1260 °C (Manufacturer: Unifrax Corporation, Niagara Falls, NY).
- The igniter used has a power supply of 117 V and 10 mA firing at a rate of 4 Hz.

A36 steel is used as the burner casing material to enable good heat conduction (with thermal conductivity $k = 51.9$ W/(m K)) to the thermoelectric devices. The casing is split into two equal parts and is sealed with a number of screws and a high temperature gasket to allow easy replacing of the porous alumina sections, as shown in Fig. 1. Five thermocouples are located inside the metal casing within the flow, while the other two are located outside; one between the casing and the hot-side of the thermoelectric module and one on the cool-side of the thermoelectric module.

Fig. 1 shows a schematic presentation of a porous burner, in which the flame is stabilized and localized within the central higher-porosity combustion section interposed by the upstream and downstream lower-porosity sections that quench the flame. Fig. 2 shows the actual pictures of the porous burner assembly. The complete schematic of the porous burner experimental set-up is shown in Fig. 3, which includes: a) methane tank, flow controllers, variable voltage sources and tubing; b) more detailed view where an impinging jet cooling system along with insulation is shown; c) the inner part of the porous burner with two outer alumina honeycomb sections and one inner porous alumina section; and d) top view of the outer alumina.

3. Experimental design and procedure

Four different experiments were performed using the proposed burner. For the first two experiments, an Al_2O_3 porous medium was used for the combustion section, which is considered inert with no catalytic enhancement of combustion. In the first test using porous Al_2O_3 media, a stoichiometric mixture was used. In the second experiment with porous Al_2O_3, the fuel concentration was periodically reduced in order to determine the lower-limit of the fuel-to-air ratio. After these two Al_2O_3 porous medium experiments were performed, the alumina combustion section was dip-coated with SiC powder, which was then tested as a possible catalytic enhancement of the combustion reaction. In the experiments with the alumina combustion section coated with SiC coating, both a stoichiometric and a lean mixture ratio was used to determine the lean flammability limit. The 6H-SiC powder (UF-10, H. C. Stark) was chosen as a catalytic enhancement mainly because of the low cost of the material, its broad availability, and its unexplored catalyticity in the combustion reaction.

3.1. Experimental procedure

The porous burner was run with a stoichiometric mixture of methane and air at the predetermined total flow rate of 11.5 L/min for the inert Al_2O_3 central section. The burner was allowed to run until it reached a steady-state temperature, which was used to create base-line results for the operational parameters of the burner. After reaching the steady-state condition, the fuel concentration was periodically decreased. The inlet air flow was increased alongside a decreasing methane content thereby keeping the total flow rate constant. The concentration was reduced every ten minutes, allowing the burner's temperature to plateau at the new concentration before further decreasing. This process was continued until it was seen that the temperatures within the burner were not sustainable (that is decreasing with time and not steady) at the given fuel concentration, thereby establishing the lean operation limit of the burner. When possible, after each temperature fall-off, the concentration was immediately increased so that a flame could be re-established for a desirable next run.

The burner was then tested with the sections coated with 6H-SiC ceramics. First, a base-line test was performed with a stoichiometric mixture and allowed to reach a steady-state temperature. Another test was performed with the coated section, during which the concentration was reduced as much as possible to determine the lean limit of the burner with the coated section.

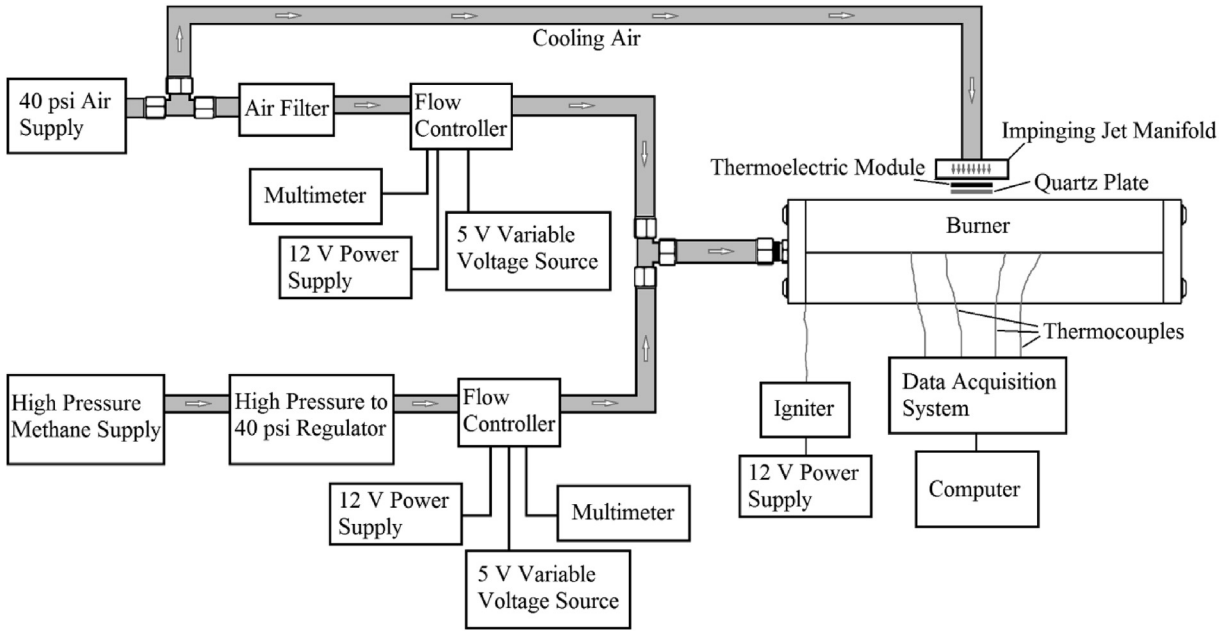

Fig. 3. Top: Burner set-up including methane tank, flow controllers, variable voltage sources and tubing; Bottom: Schematic drawing of burner set-up.

3.2. Catalyst coating

The 6H-SiC catalytic powder of interest was coated on the central porous Al_2O_3 section using a dip-coating technique. Dip-coating is a very simple slurry-coating technique which refers to: a) immersing a sample (in this case a porous ceramic foam) into a tank containing a slurry with the coating material; b) keeping the sample in the slurry for a specific amount of time (60 s), allowing the coating to penetrate the pores and bond to the surface; and c) removing the sample from the tank and allowing the sample with coating to drain and dry. Dip-coating is very straightforward and is the most suitable technique for this purpose since the porous structure and its surface are difficult to coat using other methods, such as spray deposition or sputter-coating. Immersing the matrix in the slurry ensured that all, or almost all, of the surface would be covered with coating. Complete covering of the interior surface of the combustion section depends on the viscosity of the slurry in the dip tank. The dip-coating solution is made by mixing the ceramic powder with propan-2-ol. Efficient mixing of ceramic powder with a solvent was performed using ultrasound, which allowed the formation of a homogeneous and stable suspension. In order to determine the coating load of the porous burner with a ceramic coating, the weight of the porous combustion section was measured before and after each deposition. If the coating thickness/loading was too little, then repetitive dipping into the slurry was be made, with each dipping followed by slow drying, over 24 h, to ensure that there is no spallation and delamination of the coating layers after deposition. The goal is to develop a homogenous porous coating with high specific surface area strongly attached to the surface of the porous matrix. Two different combustion sections were dip-coated with SiC as shown in Fig. 4. A photograph of the alumina section before dip-coating is shown in Fig. 4A and the section after dip-coating with deposited SiC is shown in Fig. 4B. A mixture composed of 45 g of 6H-SiC powder to 100 mL of propan-2-ol was used in the testing. Alumina sections were dip-coated, covered and allowed to dry for 24 h. A second dip-coating was deemed necessary for an even and complete deposition of the catalyst. Weight measurements were taken with just the initial alumina sections and then after the first and second dip-coating, in order to determine how much of the catalyst was deposited. The values that were obtained have been listed in Table 2, where results of two different samples are shown. On average, the coating made up about 12% of the total weight of the burner's porous ceramic chamber.

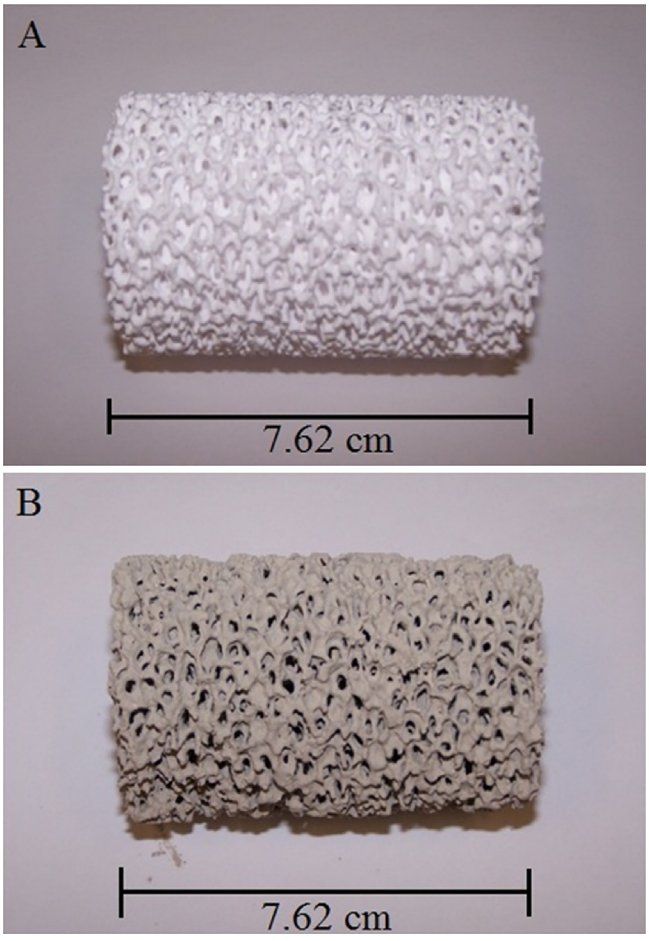

Fig. 4. Photographs of inert alumina section and SiC coated section.

Table 1
Detailed thermocouple placement locations.

Data set label	Thermocouple location
Input 0	Before inlet honeycomb section, 12.7 mm (1/2 the radius) out from the radial center
Input 1	Between the inlet honeycomb and the central foam section, 12.7 mm (1/2 the radius) out from the radial center
Input 2	Between the central foam section and the exit honeycomb, placed at the radial center
Input 3	Below the central foam section, direct bottom middle of the combustion chamber
Input 4	Above the central foam section, direct top middle of the combustion chamber
Input 5	Outside of the burner casing, middle of the top surface, underneath thermoelectric device
Input 6	Top (cold) side of the thermoelectric device

3.3. Catalyst characterization

Both the inert alumina combustion and the dip-coated combustion sections were characterized using Scanning Electron Microscopy (SEM, Ultra-55, Zeiss, USA). The surfaces were characterized at two different magnifications both before and after the combustion reaction to determine the quality of the surface and to detect changes which would help to clarify how the material affected combustion. Grain size and inhomogeneity in the material were evaluated with particular interest in the microstructural changes in the porous media surfaces as a result of combustion.

The micrographs of uncoated alumina surfaces before combustion are shown in Fig. 5A and B, and Fig. 5C and D shows the results after testing. The surface of alumina (Fig. 5A) shows a rather homogeneous grain size and grain size distribution with no excessively large grains present. The surface-termination steps can be found at the surface of alumina and more morphological features of the grains can be seen in Fig. 5B. As shown by the figure, the overall alumina surface was clean from external impurities with no deposits found. After testing of the porous combustion section in the burner, certain amounts of unknown deposits were detected, as shown in Fig. 5C and D.

Table 2
Dip-coating weights (in g).

Section #	Before dip-coating	After 1st coat	After 2nd coat	Deposited Catalyst	% of total
1	108.95	115.01	121.20	12.25	10.12
2	120.66	130.29	139.70	19.04	13.63

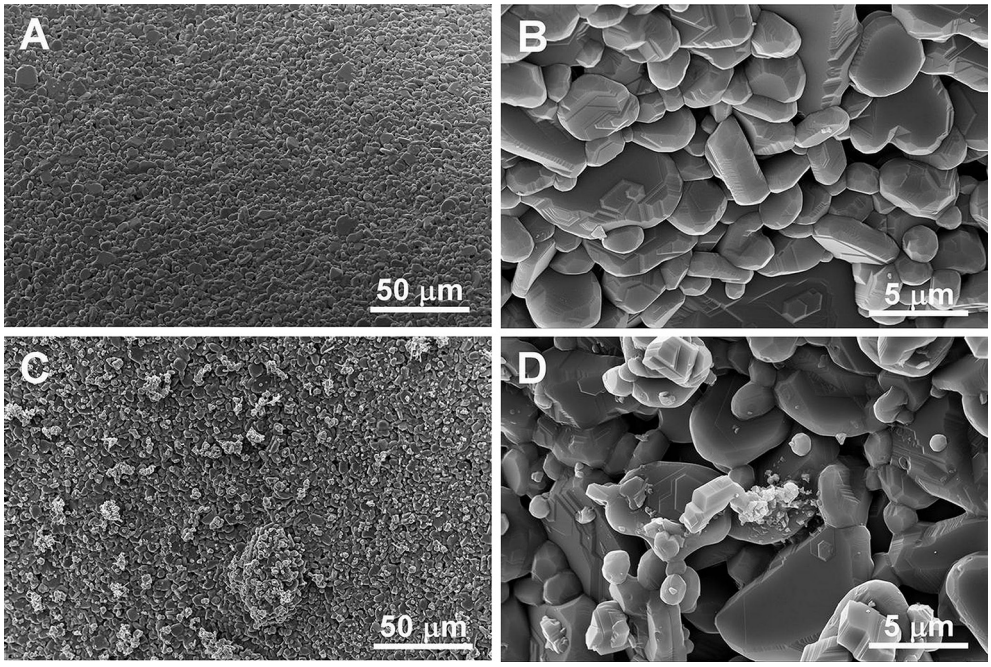

Fig. 5. SEM pictures of Al_2O_3: before use (A and B) and after use in the combustion chamber (C and D).

The surfaces of the porous media after dip-coating with the catalytically active SiC ceramic layers are shown in Fig. 6. While grain size of alumina without coating is rather large (3–5 micron, as shown in Fig. 5B), the particles of SiC powder are all in the range of less than 1 μm (Fig. 6B). Furthermore, one can see that the alumina surface is homogeneously coated with SiC before testing (Fig. 6A). Some contamination and non-homogeneous areas are visible after combustion with no clear deposits (Fig. 6C), but at higher magnification one can see that morphology of the SiC fine grains has slightly changed from irregular sharp corner shapes in the unused section (Fig. 6B) to a more smooth and rounded morphology once the grain particles were exposed to the combustion (Fig. 6D). This may result from the fact that the SiC surface was oxidized and the SiO_2 layers were formed on the surface of SiC particles. More research has to be performed for a more detailed characterization of SiC particles after combustion.

4. Testing results of porous burner

The burner was first run with the inert porous alumina section to obtain a base-line result. For the base-line test, a stoichiometric mixture of methane and air was used. The temperature time-trace

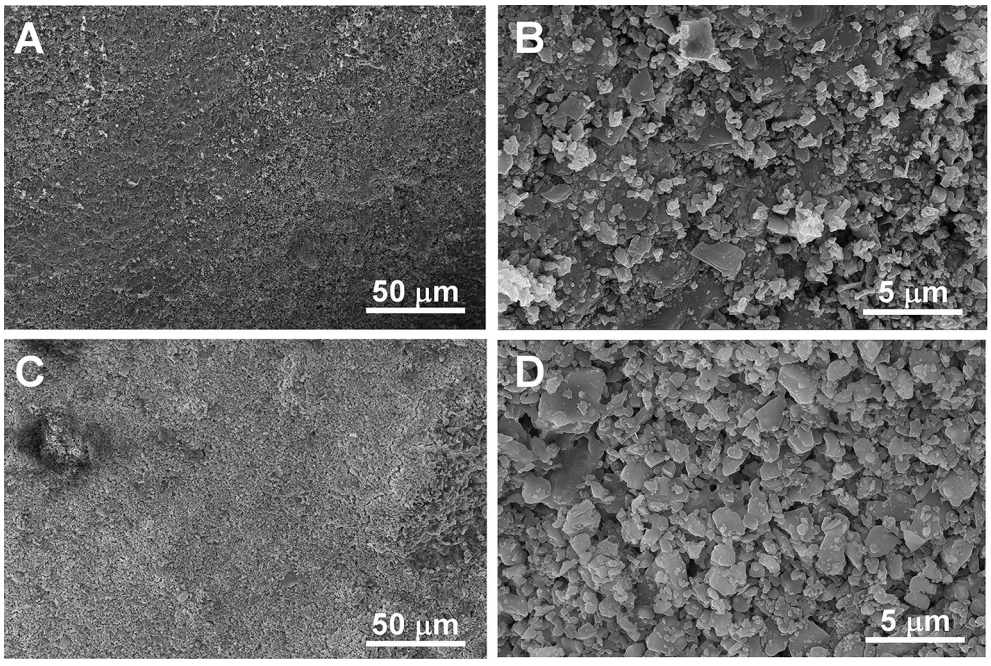

Fig. 6. SEM pictures of SiC coated Al_2O_3: before use (A and B) and after use in the combustion chamber (C and D).

for the seven thermocouples (locations described in Table 1 and pictured in Fig. 1) is shown as Fig. 7A. The thermocouple between the inlet and central sections recorded a maximum steady-state temperature of 480 °C. The steady-state temperature on the hot-side and cold-side of the thermoelectric device was 225 °C and 61 °C (outputs from Thermocouples 5 and 6, respectively), respectively, giving a temperature difference of $\Delta T = 164$ °C. The burner took approximately 3 h to reach its steady-state temperature (it is noted that the temperature drop-off after 3 h was due to shut-off of the operation). The extended period of time required to spread the flame and develop a full combustion zone can be explained by the ignition technique applied in these experiments. The spark was produced by the igniter located at the beginning of the inlet honeycomb structure (Fig. 3). The spark was produced periodically to ignite the stoichiometric gas mixture, which initially became extinguished, however during the ignition a heat wave was generated and further absorbed by the adjacent porous media. Once the significant number of ignitions occurred, the sufficient preheated volume was generated in the system at the certain adequate temperature, allowing for the next spark to ignite and develop a full combustion zone. The associated power plot for the inert section run at stoichiometric conditions is presented in Fig. 7C. The maximum load current for this run was measured to be 374 mA, as shown in Fig. 7C. The maximum load voltage was measured to be 486 mV. The peak power output achieved was 181 mW. The burner was run again with the inert porous section, but the methane concentration was now incrementally decreased to try to obtain the lean limit. The temperature time-trace is shown in Fig. 7B. The burner was again allowed to reach a near steady-state temperature of about 480 °C at stoichiometric conditions, which occurred at approximately 2 h, before the concentration was decreased. The associated power plot is shown as Fig. 7D. The maximum measured load current was 193 mA. The maximum measured load voltage was 0.964 V. The peak power was 181 mW. At an equivalence ratio of 0.589, a steady-state temperature is possible to achieve, but at an equivalence ratio of 0.579, the temperature continues to drop at a rate of 3.41 °C/min and combustion is not sustainable.

The burner was then run with one of the dip-coated combustion sections with deposited SiC coating at a stoichiometric inlet mixture. For this run, dip-coated section #1 from Table 2 was used. The burner was allowed to reach a steady-state temperature with a stoichiometric mixture, which took approximately 5.5 h, as shown in Fig. 8A. The longer time required to reach a steady-state temperature in the matrix with SiC coating in comparison with the uncoated porous Al_2O_3 matrix can be explained by the decrease in the pore size and decrease in the porosity of the combustion section of the burner due to the deposition of the coating, as well as that some pores might have become clogged during the deposition of the slurry. As a result, it was difficult for the flame to start propagation and initiate a large combustion zone, which is reflected in the appearance of the low temperature for a significant period of time. After about 2.5 h, the cooling air flow for the cool-side of the thermoelectric module was turned off, as seen by the increase in the temperatures of Input5 and Input6, since it was possible that too much heat was being extracted from the system to achieve stable combustion. After about an hour, the temperature suddenly increased, similar to the previous runs, and the cooling was turned back on while the burner approached a steady-state temperature. The maximum steady-state temperature achieved was 544 °C between the upstream and combustion sections, Input1. The hot-side of the thermoelectric device reached 181 °C and the cold-side reached 53 °C for a $\Delta T = 128$ °C. The hot-side of the thermoelectric device was notably lower than in previous uncoated runs, even though the maximum temperature was larger suggesting a difference in either flame location or thermal conductivity through the matrix. The top-side of the central section within the burner, just below the thermoelectric device, achieved a

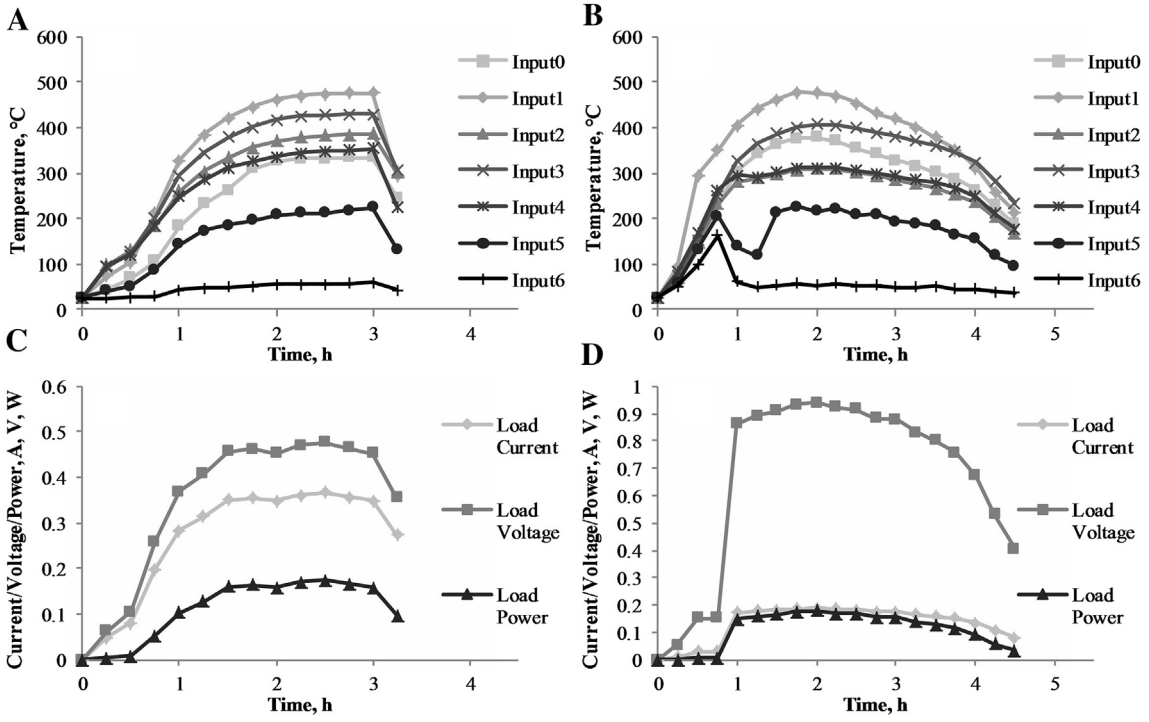

Fig. 7. Temperature and power profiles for inert Al_2O_3 section of combustor under stoichiometric and lean conditions. (A) A temperature profiles using a stoichiometric mixture of methane and air; (B) a temperature profiles using a decrease of methane concentration to achieve the lean limit; (C) a power produced during the run using the stoichiometric methane to air mixture; (D) a power produced during the run with decreasing methane concentration.

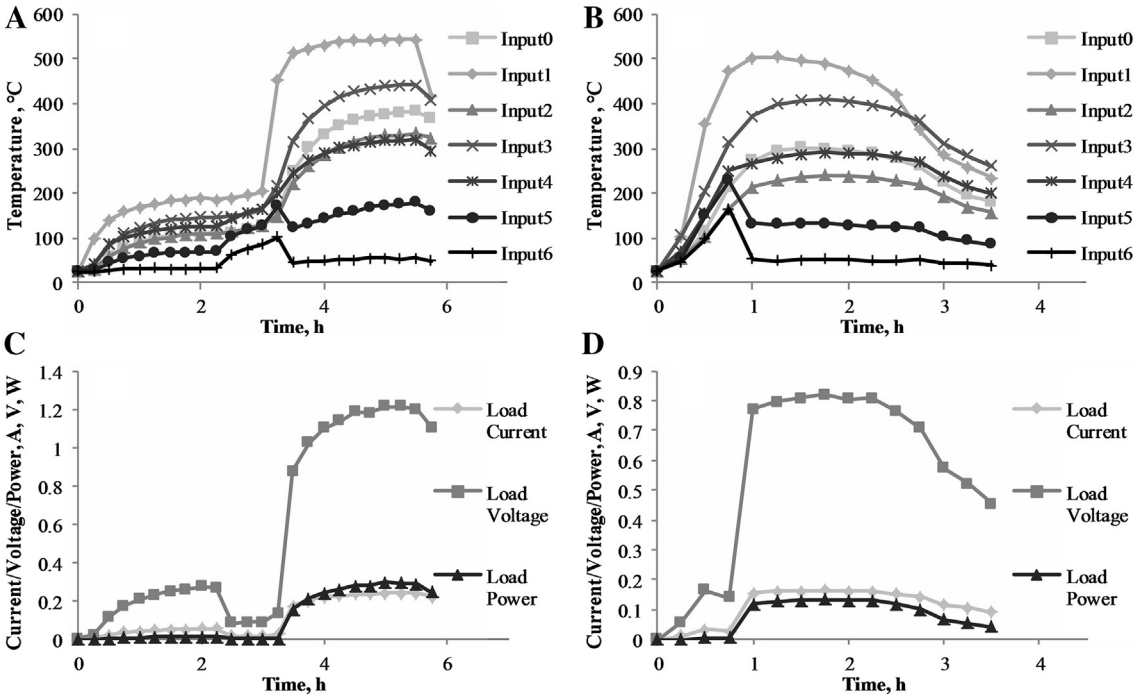

Fig. 8. Temperature and power profiles for SiC coated section of combustor under stoichiometric and lean conditions. (A) A temperature profiles using a stoichiometric mixture of methane and air; (B) a temperature profiles using a decrease of methane concentration to achieve the lean limit; (C) a power produced during the run using the stoichiometric methane to air mixture; (D) a power produced during the run with decreasing methane concentration.

maximum temperature 322 °C. For the stoichiometric test with an inert central section, this location reached a maximum temperature of 355 °C, which may account for part of the 40 °C difference on the hot-side of the thermoelectric. Fig. 8C is the associated power plot with maximum load current of 249 mA, maximum measured load voltage of 1.246 V, and peak power output of 311 mW, which is approximately 60% higher than the 181 mW output from the non-catalyzed alumina burner reported in Fig. 7C. Since the measurements prior to reaching the lean limit were done while reducing the equivalence ratio, the spotting of the time for the given equivalence ratio may not be consistent throughout this study. This may explain why a lower ΔT leads to a higher power output (Fig. 7).

The burner was also tested with a porous combustion section having a SiC catalytically active deposition to determine its lean operation limit. For this run, dip-coated section #2 from Table 2 was used. The burner was allowed to reach a peak temperature of 508 °C at stoichiometric conditions before the cooling was turned off and the mixture ratio was decreased in periodic intervals. Fig. 8B shows the temperature time-trace for this run. The burner took about one hour to reach its near-peak temperature at stoichiometric conditions. Fig. 8D shows the corresponding power plot. The peak measured load current was 165 mA. The maximum measured load voltage was 0.825 V. The peak power was 136 mW. The equivalence ratio of the inlet mixture was reduced to determine a lean operating limit for the burner with a coated center section. A stable temperature at an equivalence ratio of 0.651 was obtained. The temperature was declining by 5.14 °C/min when the equivalence ratio was reduced to 0.631. The concentration was increased back up to 0.692, allowed to reach a steady level, and then further reduced. At an equivalence ratio of 0.634, the temperature remained level. The temperature decreased by 2.03 °C/min at an equivalence ratio of 0.631. We can infer that the lean limit for the burner with a catalytically coated central section was 0.634.

The minimum achieved lean limit for the inert Al_2O_3 porous section was at an equivalence ratio of 0.589 and for the catalytically 6H-SiC coated porous section was 0.634. The overall conversion efficiency, measured as the ratio of the stored chemical energy of the incoming fuel that is converted into electrical output of the thermoelectric module of the burner system, was calculated for operation with inert and catalytic central sections at both stoichiometric mixture and the lean limit (Table 3). The input chemical energy was calculated while assuming a complete combustion reaction, the listed stoichiometric or lean limit mixture ratio, a heat of combustion of 55.6 MJ/kg, a density of 0.668 kg/m^3 at NTP (20 °C, 1 atm) conditions [29], and an inlet total flow rate of 11.5 L/min. The inert porous section at a stoichiometric inlet mixture had the largest hot-side temperature and temperature difference across the thermoelectric generator, and was closest to the manufacture's specifications but did not produce the most power. The catalytically coated section at a stoichiometric mixture had the greatest overall efficiency of 0.046% even though it had a lower $\Delta T = 128$ °C across the thermoelectric module, lower than that produced by the non-catalytic burner. Both inert and coated sections, during their lean limit tests, had low peak temperatures and, therefore, low temperature difference over the thermoelectric and generated the least amount of power.

Table 3
Overall conversion efficiency.

Test conditions	Equivalence ratio	Input chemical energy (W)	Output electrical energy (mW)	Conversion efficiency (%)
Al_2O_3, inert, stoichiometric mixture	1.000	676.88	181	0.027
Al_2O_3, inert, lean mixture	0.589	414.86	145	0.035
SiC, catalytic, stoichiometric mixture	1.000	676.88	311	0.046
SiC catalytic, lean mixture	0.634	444.35	46	0.010

5. Conclusions

The first attempts to design, assemble, and test a super-adiabatic combustor coupled with a thermoelectric module have been reported. The super-adiabatic highly-porous (80% porosity) alumina chamber with a pore size of 3–4 mm was used as a central combustion section interposed by honeycomb structures to stabilize the combustion zone in the porous section. The material of the central combustion section was either a pure Al_2O_3 or, in order to test the catalytic enhancement of the alumina surface, Al_2O_3 with a coating of catalytic SiC. Combustion with stoichiometric and lean mixtures was performed. The minimum achieved lean limit for the inert porous section was at an equivalence ratio of 0.589 and was 0.634 for the SiC coated combustion section. The results obtained show that SiC might be a good promoter of the combustion for the stoichiometric fuel-to-air ratio, but SiC coated porous media did not outperform the inert Al_2O_3 matrix where the lean mixtures were used. Power was harvested from the generated heat by the thermoelectric module mounted on the top of the steel casing. It was found that an optimal efficiency was obtained with the SiC coated combustion sections near a stoichiometric mixture and that the uncoated inert combustion section was more efficient near its lean limit than at a stoichiometric mixture.

Acknowledgements

This work was supported by NSF CMMI projects #0968911 and 1030833 and in part by ACS PRF #51768-ND10. This research was partly supported by Grant FONDECYT 1090550 awarded to Valeri Bubnovich by the Chilean government. Oliver Waters's work was supported by NSF DUE 0525429, STEM Talent Expansion Program (STEP) Type 1a: UCF STEP Pathways to STEM: From Promise to Prominence (EXCEL). We would like to thank the team of senior design undergraduate students, Naseer Ahmed, Maricela DeSantiago, John Gintert and Maulik Shah for their work on the construction of the burner.

References

[1] Mujeebu MA, Abdullah MZ, Abu Bakar MZ, Mohamad AA, Muhad RMN, Abdullah MK. Combustion in porous media and its applications – a comprehensive survey. J Environ Manage 2009;90:2287–312.
[2] Keramiotis C, Stelzner B, Trimis D, Founti M. Porous burners for low emission combustion: an experimental investigation. Energy 2012;45:213–9.
[3] Delalic N, Mulahasanovic Dz, Ganic EN. Porous media compact heat exchanger unit – experiment and analysis. Exp Therm Fluid Sci 2004;28:185–92.
[4] Hanamura K, Echigo R, Zhdanok SA. Superadiabatic combustion in a porous medium. Int J Heat Mass Transf 1993;36:3201–9.
[5] Kennedy LA, Fridman AA, Saveliev AV. Superadiabatic combustion in porous media: wave propagation, instabilities, new type of chemical reactor. Int J Fluid Mech Res 1995;22:1–26.
[6] Mujeebu MA, Abdullah MZ, Mohamad AA. Development of energy efficient porous medium burners on surface and submerged combustion modes. Energy 2011;36:5132–9.
[7] Mohamad AA. Ingham DB, Pop I, editors. Transport phenomena in porous media III. Oxford, UK: Elsevier Science; 2005. p. 287–304.
[8] Lloyd SA, Weinberg FJ. A burner for mixtures of very low heat content. Nature 1974;251:47–9.
[9] Weinberg FJ. Combustion temperatures: the future? Nature 1971;233:239–41.
[10] Pickenäcker O, Pickenäcker K, Wawrzinek K, Trimis D, Pritzkow WEC, Müller C, et al. Int Ceram Rev 1999;48:326–9. 424–34.
[11] Fend T, Trimis D, Pitz-Paal R, Hoffschmidt B, Reutter O. Thermal properties. In: Cellular ceramics: structure, manufacturing, properties and applications. Weinheim, Germany: Wiley-VCH Verlag GmbH; 2005. p. 342–60.
[12] Hardesty DR, Weinberg FJ. Burners producing large excess enthalpies. Combust Sci Technol 1974;8:201–14.
[13] Wood V, Harris AT. Porous burners for lean-burn applications. Prog Energy Combust Sci 2008;34:667–84.
[14] Hanamura K, Kumano T, Iida Y. Electric power generation by superadiabatic combustion in thermoelectric porous element. Energy 2005;30:347–57.
[15] Katsuki F, Tomida T, Nakatani H, Katoh M, Takata A. Development of a thermoelectric power generation system using reciprocating flow combustion in a porous $FeSi_2$ element. Rev Sci Instrum 2001;72:3996–9.
[16] Ismail AK, Abdullah MZ, Zubair M, Ahmad ZA, Jamaludin AR, Mustafa KF, et al. Application of porous medium burner with micro cogeneration system. Energy 2013;50:131–42.
[17] Avdic F, Adzic M, Durst F. Small scale porous medium combustion system for heat production in households. Appl Energy 2010;87:2148–55.
[18] Babkin VS, Laevskii YM. Seepage gas combustion. Combust Explo Shock Waves 1987;23:531–47.
[19] Tritt TM. Thermoelectric phenomena, materials, applications. Annu Rev Mater Res 2011;41:433–48.
[20] Ellzey JL, Goel R. Emissions of CO and NO from a two stage porous media burner. Combust Sci Technol 1995;107:81–91.
[21] Yu B, Kum S-M, Lee C-E, Lee S. Combustion characteristics and thermal efficiency for premixed porous-media types of burners. Energy. http://dx.doi.org/10.1016/j.energy.2013.02.035; 2013.
[22] Rortveit GJ, Zepter K, Skreiberg O, Fossum M, Hustad JE. Proc Combust Inst 2002;29:1123–9.
[23] Trimis D, Durst F. Combustion in porous medium – advances and applications. Combust Sci Technol 1996;121:153–68.
[24] Bowen HK. Basic research needs on high temperature ceramics for energy applications. Mater Sci Eng 1980;44:1–56.
[25] Howell JR, Hall MJ, Ellzey JL. Combustion of hydrocarbon fuels within porous inert media. Prog Energy Combust Sci 1996;22:121–45.
[26] Ambrogio M, Saracco G, Specchia V. Combining filtration and catalytic combustion in particulate traps for diesel exhaust treatment. Chem Eng Sci 2001;56:1613–21.
[27] Vogt UF, Gyorfy UF, Herzog A, Graule T, Plesch G. J Phys Chem Solids 2007;68:1234–8.
[28] Hsu P-F, Evans WD, Howell JR. Experimental and numerical study of premixed combustion within nonhomogeneous porous ceramics. Combust Sci Technol 1993;90:149–72.
[29] Glassman I, Yetter RA. Combustion. 4th ed. Burlington, MA, USA: Elsevier Inc.; 2008.